Graphical Abstract



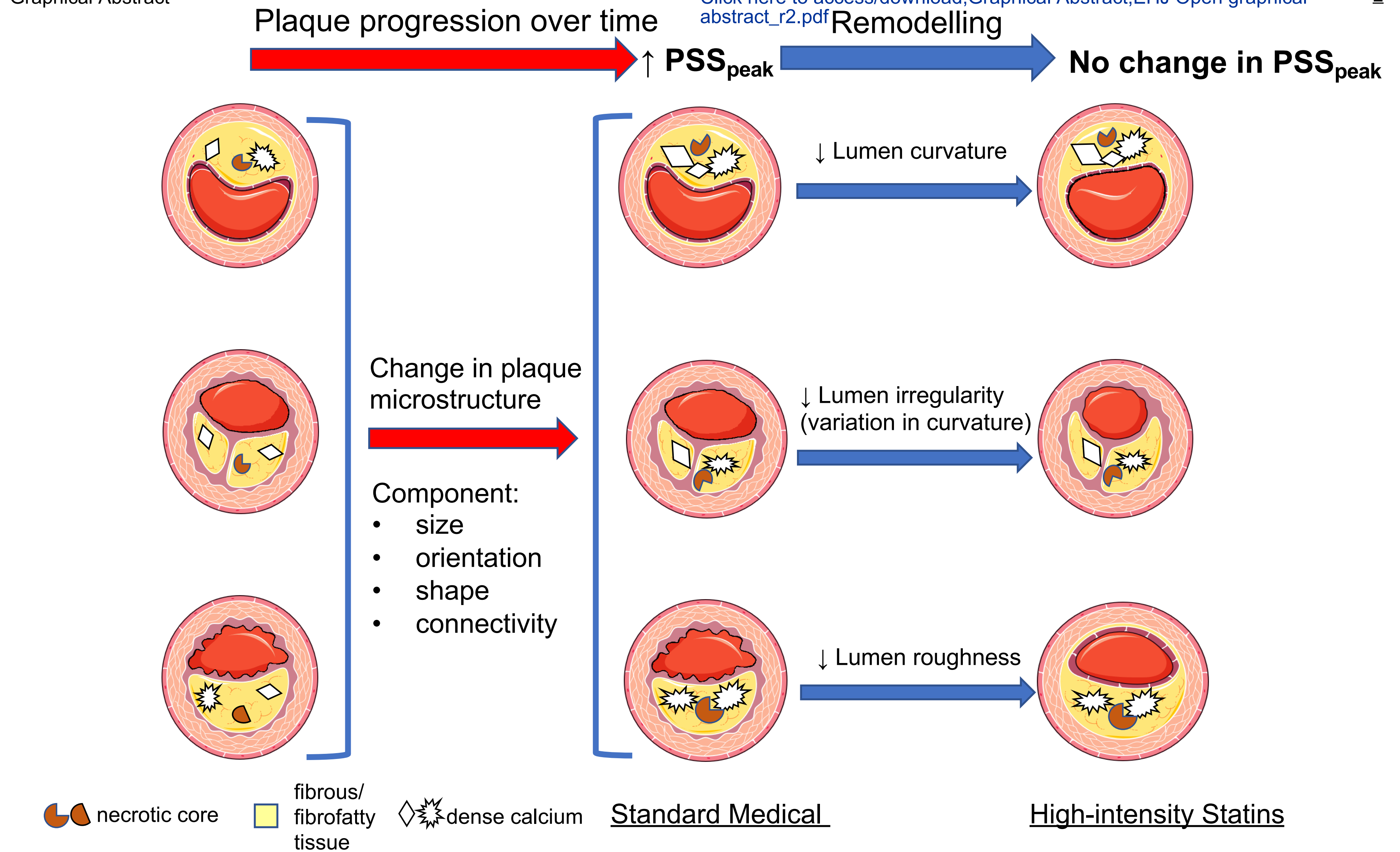


**Graphical abstract**

Plaques progress over time with standard medical treatment due to changes in plaque microstructure, resulting in increased peak plaque structural stress (PSS) in advanced lesions. High-intensity statin treatment is associated with remodelling of the lumen/plaque interface, reducing lumen curvature, irregularity and roughness, and preventing the increase in peak PSS seen with standard medical treatment. Smoothing plaques and reducing lumen curvature may represent novel mechanisms whereby high-intensity statins may protect against plaque rupture.

# High-intensity Statin Treatment Is Associated with Reduced Plaque Structural Stress and Remodelling of Artery Geometry and Plaque Architecture

Short running title: High-intensity Statins and Structural Stress

Sophie Z. Gu[1], Charis Costopoulos[2], Yuan Huang[3,4], Christos Bourantas[5,6], Adam Woolf[1], Chang Sun[4], Zhongzhao Teng[4,7], Sylvain Losdat[8], Lorenz Räber[9], Habib Samady[10], and Martin R. Bennett[1]*

[1]Division of Cardiovascular Medicine, University of Cambridge, Level 6, ACCI, Hills Road, Addenbrooke's Hospital, Cambridge, CB2 0QQ, UK
[2]Department of Cardiology, Royal Papworth Hospital, Papworth Road, Cambridge, CB2 0AY, UK
[3]Centre for Mathematical and Statistical Analysis of Multimodal Imaging, University of Cambridge, 20 Clarkson Road, Cambridge, CB3 0EH, UK
[4]Department of Radiology, University of Cambridge, Hills Road, Addenbrooke's Hospital, Cambridge, CB2 0QQ, UK
[5]Institute of Cardiovascular Sciences, University College London, 62 Huntley Street, London, WC1E 6DD, UK
[6]Department of Cardiology, Barts Heart Centre, West Smithfield, London, EC1A 7BE, UK
[7]Department of Engineering, University of Cambridge, Trumpington Street, Cambridge, CB2 1PZ, UK
[8]Institute of Social and Preventive Medicine and Clinical Trials Unit, University of Bern, Hochschulstrasse 6, 3012 Bern, Switzerland
[9]Department of Cardiology, Bern University Hospital, 3010 Bern, Switzerland
[10]Division of Cardiology, Department of Medicine, Emory University School of Medicine, 201 Dowman Drive, Atlanta, GA 30322, USA.

***Corresponding author:** Professor Martin R. Bennett
Division of Cardiovascular Medicine, University of Cambridge, Level 6, ACCI, Addenbrooke's Hospital, Cambridge, CB2 0QQ, UK
Tel:(44)1223 331504; Fax:(44)1223 331505
E-mail: mrb24@medschl.cam.ac.uk

Total word count: 4993
Figures: 6
Tables: 1

## ABSTRACT

**Aims:** Plaque structural stress (PSS) is a major cause of atherosclerotic plaque rupture and major adverse cardiovascular events (MACE). We examined the predictors of changes in peak and mean PSS ($\Delta PSS_{peak}$, $\Delta PSS_{mean}$) in three studies of patients receiving either standard medical or high-intensity statin (HIS) treatment.

**Methods and results:** We examined changes in PSS, plaque size and composition between 7,348 co-registered baseline and follow-up virtual-histology intravascular ultrasound images in patients receiving standard medical treatment (controls, n=18) or HIS (atorvastatin 80mg, n=20, or rosuvastatin 40mg, n=22). The relationship between changes in $PSS_{peak}$ and plaque burden (PB) differed significantly between HIS and control groups ($p<0.001$). Notably, $PSS_{peak}$ increased significantly in control lesions with PB>60% ($p=0.04$), but not with HIS treatment. However, $\Delta PSS_{peak}$ correlated poorly with changes in lumen and plaque area or PB, plaque composition or lipid lowering. In contrast, $\Delta PSS_{peak}$ correlated significantly with changes in lumen curvature, irregularity and roughness ($p<0.05$), all of which were reduced in HIS patients. $\Delta PSS_{mean}$ correlated with changes in lumen area, PA, PB, and circumferential calcification, and was unchanged with either treatment.

**Conclusion:** Our observational study shows that $PSS_{peak}$ changes over time were associated with baseline disease severity and treatment. The $PSS_{peak}$ increase seen in advanced lesions with standard treatment was associated with remodelling artery geometry and plaque architecture, but this was not seen after HIS treatment. Smoothing plaques by reducing plaque/lumen roughness, irregularity and curvature represent a novel mechanism whereby high-intensity statins may reduce PSS, and thus may protect against plaque rupture and MACE.

**Keywords:** Atherosclerosis, plaque architecture, plaque structural stress, virtual-histology intravascular ultrasound

**INTRODUCTION**

Despite current optimal medical and interventional management, patients with coronary artery disease (CAD) have significant risk of future major adverse cardiovascular events (MACE).[1,2] In particular, patients presenting with acute coronary syndrome (ACS) demonstrate multiple vulnerable plaques and simultaneous plaque ruptures in non-culprit vessels,[3] confirming the multifocal nature of unstable atherosclerosis, and prospective studies show that 50% of future MACE occur in non-culprit vessels.[4,5] Lipid-lowering with statins and proprotein convertase subtilisin kexin type 9 (PCSK9) inhibitors reduce MACE by 25%-40%,[1,2,6] despite modest reductions in lumen stenosis[7] and <1% reduction in whole-vessel percent atheroma volume (PAV),[8,9] suggesting that these drugs may stabilize plaques, for example by increasing fibrous tissue (FT) and reducing necrotic core (NC). However, virtual-histology intravascular ultrasound (VH-IVUS) studies show only small or no change in FT or NC areas after statins[10,11] or PCSK9 inhibitors,[12] suggesting that changes in plaque composition alone do not fully explain their marked clinical benefit.

Coronary plaques undergo mechanical loading due to dynamic changes in blood pressure and flow,[13] with rupture occurring if plaque structural stress (PSS) exceeds its mechanical strength. PSS can be calculated from arterial and plaque geometry, plaque composition, tissue material properties (defined from *ex vivo* tensile testing), and blood pressure. Maximal PSS ($PSS_{peak}$) is increased at higher-risk plaques in ACS vs. stable angina patients,[14] at rupture sites vs. stable lesions,[15] and plaques associated with future MACE.[16,17] Furthermore, increased baseline PSS is associated with changes to a more 'vulnerable plaque' phenotype over time.[18] However, how PSS changes over time, the major predictors of these changes, and whether lipid-lowering affects PSS are unknown. We examined changes in PSS in three studies of patients receiving either standard medical treatment or high-intensity statins (HIS).

We find that PSS increases in advanced lesions with standard medical but not HIS treatment, associated with remodelling artery geometry and plaque architecture.

## METHODS

### STUDIES

Studies were conducted at Emory University Hospital, USA and Bern University Hospital, Switzerland. All studies were approved by institutional review boards (ClinicalTrials.gov: NCT00576576, NCT01230892, NCT00962416), and all patients provided informed consent and underwent protocol-driven baseline and follow-up angiography and VH-IVUS.

Control patients received standard medical treatment, which included aspirin, low-intensity statin, and a β-blocker for 12m (n=18). HIS patients received either atorvastatin 80mg for 6m (n=20) or rosuvastatin 40mg for 13m (n=22). Control patients presented with stable angina with an abnormal non-invasive stress test, or ACS with moderate but non-obstructive lesions (plaque burden [PB]≥40%, <50% stenosis visually by angiography or <70% stenosis with FFR>0.80).[19] Atorvastatin-treated patients presented with either stable angina or ACS with moderate lesions, while rosuvastatin-treated patients presented with ST-segment elevation myocardial infarction (STEMI), with study of moderate lesions in non-culprit vessels.[20,21] We analysed only left anterior descending arteries as USA studies included only these arteries.

### VIRTUAL HISTOLOGY INTRAVASCULAR ULTRASOUND (VH-IVUS)

Images were acquired with phased-array 20-MHz Eagle Eye catheters (Volcano Corp., Rancho Cordova, USA) using 0.5mm/s automated motorized pullback. Radiofrequency data were captured on the R-wave using ECG-triggered acquisition. All images underwent quality control assessment by experienced investigators blinded to clinical data at Emory

Cardiovascular Imaging and Biomechanical Core Laboratory (control and atorvastatin) or Cardialysis B.V., Rotterdam (rosuvastatin). Data were analysed offline using echoPlaque 4.0 (Indec Medical, San Jose, USA) and QIVUS software (Medis, Leiden, Netherlands). Lumen and external elastic membrane (EEM) areas, plaque area (PA, defined as plaque and media=EEM minus lumen areas), PB (defined as 100% x PA/EEM area), plaque composition (fibrofatty [FF], fibrous tissue [FT], necrotic core [NC], and dense calcium [DC] area and percentage) were calculated between baseline and follow-up.

Baseline and follow-up VH-IVUS frames were co-registered longitudinally using anatomical landmarks (e.g., side branches, stenosis, calcification/large lipid cores). Frames were rotated using anatomical landmarks and lumen shape matching for circumferential alignment. Matching was confirmed by 2 analysts and showed good reproducibility (see **Supplementary material online**).

## LUMEN ANALYSIS

We also calculated lumen aspect ratio (ratio between maximum/minimum diameter of ellipse) to measure lumen eccentricity, lumen curvature (computed using the radius of the circle determined by the point of interest and 2 adjacent points) to measure lumen angulation, lumen irregularity (variation in luminal angulation), and lumen roughness (lumen surface evenness in respect to curvature) (**Supplemental material online, *Figure S1***).[22]

## BIOMECHANICAL ANALYSIS

Each vessel generated an average 169 (136-212) (median, interquartile range [IQR]) baseline and follow-up VH-IVUS frames (total = 10,517 frames). 4,933 frames with <30% stenosis or containing significant side branches or immediately adjacent to bifurcations were excluded from finite element analysis (FEA) due to violating the plane strain assumption for 2-dimensional (2D) solid modelling. Vessel geometry and plaque composition were extracted and 2D dynamic FEA simulations performed as described previously (**Supplementary material online)**.[16] Maximum principal stress in the peri-luminal region was used to indicate critical mechanical conditions within the structure.

## STATISTICAL ANALYSIS

As each plaque had multiple VH-IVUS frames, linear mixed-effects (LME) models were used to account for hierarchical data structure and clustering in individual patients undergoing different treatments, and results presented as mean±standard error (SE). All plaque anatomical, geometric, compositional or PSS measurements were analysed by LME on frame-based data in each patient unless otherwise indicated. Adjustment of p values for multiple comparisons was performed using the Bonferroni method. Potential confounding factors were included in multivariable regression analyses to assess robustness of the main study findings. Model diagnostics were performed by inspecting residual and Q-Q plots to test model assumptions. Outliers were removed using the median absolute deviation method (threshold 3.5). Association between continuous variables was assessed by Pearson's correlation coefficient and linear regression. Regression slopes were compared using the analysis of covariance (ANCOVA) test. Statistical significance was indicated by two-tailed p-value <0.05. Statistical Package for the Social Sciences (SPSS, version 26.0; IBM, New York, USA) and R 4.0.3 (R Foundation for Statistical Computing) were used for all statistical analyses. MRB had full access to all study data and takes responsibility for its integrity and data analysis.

## RESULTS

## STUDY POPULATIONS

We examined PSS and plaque characteristics at baseline and follow-up in patients treated with either: (1) Standard medical therapy including low-intensity statins for 12m (controls), or (2) either 80mg atorvastatin for 6m or 40mg rosuvastatin for 13m (high-intensity statins-HIS) in three separate trials (***Figure 1***). Full trial details and patient demographics are shown in **Supplementary material online, *Tables S1* and *S2***. Control and atorvastatin patients had similar baseline demographics, but more control patients had prior statin and nitrate use. The rosuvastatin group had more males and smokers, and fewer prior statin, anticoagulation or angina medications compared to controls. Low-density lipoprotein (LDL) levels increased slightly over time in control patients, most likely from patient discontinuation of standard treatment, but were reduced in atorvastatin and rosuvastatin patients; there was no difference in changes in high-density lipoprotein (HDL) levels or blood pressure reduction between groups. Baseline plaque characteristics were largely similar between control and atorvastatin patients, including VH-IVUS-determined plaque composition, but rosuvastatin patients had smaller EEM, lumen areas and FT%, and higher plaque burden but not plaque area vs. controls (**Supplementary material online, *Table S3***). We therefore co-registered images (***Figure 1***) and analysed changes between baseline and follow-up images for each treatment, with each patient acting as their own control, rather than direct comparisons between groups.

## CHANGES IN PSS WITH TREATMENT

Maximal PSS ($PSS_{peak}$) and mean PSS ($PSS_{mean}$) were calculated for each frame (total n=7,348 frames). $PSS_{peak}$ was reduced overall in control patients, but this effect was due to small lesions (PB<40%, ***Figure 2A***) whose clinical significance is unclear, as PB is a major predictor of MACE in prospective VH-IVUS trials.[4,5,23] In contrast, $PSS_{peak}$ was unchanged in moderate lesions (PB 40%-60%) in control patients, but increased significantly in

PB>60% lesions (15.6±5.3 kPa, mean±SE, p=0.04). Atorvastatin and rosuvastatin patients showed no change in $PSS_{peak}$ at any PB, and particularly no rise in $PSS_{peak}$ in PB>60% lesions (***Figure 2A***). Analysis of 2mm axial segments showed broadly similar findings (**Supplementary material online, *Table S4***), while mean PSS was unchanged in control, atorvastatin or rosuvastatin patients at any PB **(*Figure 2B*)**.

Our findings suggest that the major effect of HIS on $PSS_{peak}$ is on advanced lesions (PB>60%). We therefore used interaction plots of linear mixed-effects models to examine interaction effects of treatment group and baseline plaque burden or plaque area on changes in $PSS_{peak.}$ There was a significant interaction between $\Delta PSS_{peak}$ and PB for HIS vs. control treatments (atorvastatin vs. control, adjusted p<0.001; rosuvastatin vs. control, adjusted p<0.001), indicating the relationship between $\Delta PSS_{peak}$ and PB differed between control and atorvastatin/rosuvastatin treatments. Notably, $\Delta PSS_{peak}$ increased when PB was above ~50% in controls but was unchanged with either atorvastatin or rosuvastatin. A similar interaction effect occurred between baseline PA and treatment group, where $PSS_{peak}$ increased when PA was above ~8.0mm$^2$ in controls, and not with atorvastatin/rosuvastatin (***Figure 2C-D***).

To examine whether the relationship between PSS and PB/PA or treatment was due to differences in patient demographics, we undertook multivariable analyses of potential clinically-important confounding factors such as age, gender, hypertension, smoking status, diabetes, family history of CAD and prior statin use. Despite differences in these parameters between groups, the interaction effect between atorvastatin/rosuvastatin treatment and plaque burden remained (***Table 1***).

We also examined the relationship between changes in PSS and changes in serum lipids. The effects of systemic lipid lowering on individual lesion PSS are not predictable, as $PSS_{peak}$ varies markedly between frames[17] and is highly localized to specific plaque regions related to both architecture and geometry, while $PSS_{mean}$ averages values around the lumen circumference (***Figure 1D***). Changes in $PSS_{peak}$ and $PSS_{mean}$ were only weakly (and negatively) correlated with LDL changes in individual patients (and not correlated with changes in HDL)(**Supplementary material online, *Figure S2***), suggesting that LDL reduction alone is not associated with reduced PSS.

**EFFECTS OF CHANGES IN PLAQUE COMPOSITION, AND GEOMETRY**

We next examined whether changes in peak and mean PSS with treatment were associated with changes in plaque geometric and compositional parameters. Control patients showed no significant change in any plaque characteristic. Atorvastatin-treated patients had reduced FF area and %, and FT area, and increased DC area and %. Rosuvastatin-treated patients showed decreased EEM, plaque, and FT areas, and increased DC % (***Figure 3***). However, $\Delta PSS_{peak}$ was only weakly correlated with Δlumen area, ΔPA or ΔPB in all plaques, although more strongly correlated with Δlumen aspect ratio, a measure of lumen 'roundness'; in contrast, $\Delta PSS_{mean}$ was positively correlated with increasing lumen area and decreasing PA or PB, but not Δlumen aspect ratio (**Supplementary material online, *Table S5***). Both $\Delta PSS_{peak}$ and $\Delta PSS_{mean}$ also correlated poorly with changes in NC, FF or FT areas or percentage, suggesting that effect of HIS on $PSS_{peak}$ is not due to different effects on plaque composition alone. $\Delta PSS_{peak}$ was poorly correlated with calcification, although $\Delta PSS_{mean}$ was more strongly correlated with ΔDC area, ΔDC maximum and total arcs.

We further examined whether changes in plaque areas or components explain $PSS_{peak}$ differences in PB>60% lesions between control and HIS treatments. Although changes in plaque area, burden or specific component parameters were significantly different between baseline and follow-up in control or atorvastatin/rosuvastatin patients, the direction of changes was similar in all groups (***Figure 4***). This indicates that different effects on plaque or component areas alone cannot explain why $PSS_{peak}$ does not rise in PB>60% lesions with HIS treatment.

## EFFECTS OF CHANGES IN LUMEN GEOMETRY

Our data suggest that changes in $PSS_{peak}$ reflect more localized changes in lumen and plaque geometry and plaque architecture, particularly at or close to the lumen/plaque interface. We therefore explored the effect of lumen curvature, lumen irregularity, and lumen roughness on PSS in PB>60% lesions, and their changes associated with treatment. Lumen curvature, irregularity, and roughness were all strongly positively correlated with $\Delta PSS_{peak}$ but poorly with $\Delta PSS_{mean}$ in PB>60% lesions (***Figure 5A-C***). As regression slopes of these lumen parameters with $\Delta PSS_{peak}$ were similar (p>0.05) in atorvastatin and rosuvastatin groups (**Supplementary material online, *Figure S3)***, we examined changes in these parameters in a combined HIS treatment group vs. controls. High-intensity statins were associated with a significant reduction in lumen curvature, irregularity and lumen roughness, an effect not seen in controls (***Figure 5D)***, with similar findings 4mm proximal/distal to the minimal luminal area (MLA), a region highly correlated with MACE[17] (**Supplementary material online, *Table S6***).

## EFFECTS OF COMBINATIONS OF FACTORS ON $\Delta PSS_{peak}$ AND $\Delta PSS_{mean}$

While $\Delta PSS_{mean}$ was mostly determined by anatomical factors and circumferential calcification, and $\Delta PSS_{peak}$ by localized luminal features, these parameters may all change together. Indeed, large increases or decreases in $\Delta PSS_{mean}$ and $\Delta PSS_{peak}$ occurred when changes in multiple features coincided across a range of PB (***Figure 6***). For example, increased $PSS_{peak}$ was associated with increased lumen curvature and loss of 'shielding' calcification **(*Figure 6A*)**, and increased lumen irregularity, roughness and shoulder curvature **(*Figure 6B*)**, while decreased $PSS_{peak}$ was associated with reduced lumen irregularity, roughness and curvature, and increased confluence of superficial calcification **(*Figure 6C*)**.

## DISCUSSION

We undertook an observational study of three longitudinal trials of standard medical or high-intensity statin treatment, examining changes in PSS, plaque and lumen geometry and composition. We show that: (1) $PSS_{peak}$ increased markedly in advanced lesions with standard medical but not high-intensity statin treatment; (2) changes in $PSS_{peak}$ were associated with both treatment and plaque burden; (3) changes in plaque and lumen area or plaque composition alone do not explain potential protective effects of high-intensity statins on $\Delta PSS_{peak}$; (4) $\Delta PSS_{peak}$ is also affected by localized changes in plaque and lumen geometry, including lumen curvature, irregularity and roughness, while $\Delta PSS_{mean}$ is associated with changes in lumen and plaque areas and circumferential calcification; and (5) high-intensity statin treatment is associated with remodelling lumen and plaque shape and architecture.

Previous landmark trials found that rosuvastatin 40mg or atorvastatin 80mg for 24m reduce percent atheroma volume by only ~1%.[7,24] Similarly, although differences exist between individual VH-IVUS studies, two meta-analyses showed only small or no change in FT or

NC areas after statin treatment[10,11]. Consistent with these meta-analyses, high-intensity statin treatment was not associated with reduced PB, and patients receiving standard medical or high-intensity statin treatment showed similar changes in necrotic core and fibrofatty tissue area or %. Together, these findings suggest that small reductions in atheroma volume or these plaque components may not fully explain the ability of high-intensity statins to reduce MACE compared to standard therapy. In contrast, $PSS_{peak}$ increased significantly in PB>60% lesions with standard treatment but not high-intensity statins, an action predicted to stabilize these higher-risk plaques.

Prospective natural history VH-IVUS studies showed that PB≥70%, MLA<4mm and VH-IVUS-defined thin cap atheromas were associated with future MACE;[4,5,23] however, the overall low event rates suggest that factors additional to plaque size, stenosis and composition determine rupture. PSS measurements integrate effects of plaque anatomy and composition with physical forces, and inclusion of PSS measurements improve future MACE prediction,[16,17] especially in higher-risk regions. We therefore identified the parameters associated with changes in both mean and peak PSS. $\Delta PSS_{mean}$ correlated with changes in lumen and plaque area and PB, consistent with Laplace's law where mean wall stress increases with intracavity pressure or increasing vessel radius (when plaques regress) or vice versa (when plaques progress). $\Delta PSS_{mean}$ also correlated with circumferential calcification, which can act as either stress amplifiers or lumen cap protectors depending on size, orientation, and confluence. Larger calcification plates (>1mm) may stabilize plaques by shielding from luminal stress,[25] and atorvastatin/rosuvastatin increased DC percentage, a feature shown consistently in statin trials.[10,11] Current algorithms for total DC area, arc or contour lack the ability to detect subtle changes in plaque microstructure. In contrast, PSS estimation at higher-risk plaque regions represents an objective method to quantify microstructural differences.

$PSS_{peak}$ is normally located in the superficial 0.2 mm of the lesion,[14] and at maximum curvature at the plaque shoulder, a frequent site of rupture.[26] $\Delta PSS_{peak}$ also correlated with changes in lumen curvature, irregularity and roughness, which measure both large and small lumen/plaque irregularities. These parameters were reduced in PB>60% lesions of patients receiving high-intensity statins, potentially explaining the absence of a $PSS_{peak}$ rise seen with HIS treatment. Plaque/luminal irregularity, defined as a rough lumen surface along the direction of blood flow, is a strong predictor of plaque instability,[22] while repetitive silent rupture or erosion may generate new areas of acute angulation and roughness.

The mechanisms by which high-intensity statins might reduce or prevent a rise in $PSS_{peak}$ are not known, and may be multiple. We found a weak negative correlation between ΔPSS and ΔLDL, and the interaction effect of baseline PB and treatment group on PSS was independent of prior statin use, suggesting that LDL lowering alone does not reduce PSS. However, statins also increase nitric oxide (NO) bioavailability, which improves endothelial cell function,[27] suppresses coagulation by inhibiting platelet adhesion and aggregation,[28] and blocks endothelial cell apoptosis.[29] Improved endothelial function and better reorganization of luminal thrombus may also smooth the plaque surface.

Our study has several limitations. First, trials were performed in two different centres at different times. However, the same VH-IVUS and PSS platforms were used throughout, so comparable images and PSS calculations were obtained. Second, patient demographics and plaque characteristics were not propensity-matched, including prior statin use, and PB and

PA differed between trials. However, we analysed changes in PSS and plaque and lumen features between baseline and follow-up in all patients where each patient acts as their own control, LDL reduction was not correlated with decreased PSS, PSS was examined across a full range of PB (reflecting real-world patient presentation), and our main findings remained after multivariable regression analysis for confounding factors. Third, VH-IVUS has well-documented limitations to identify and measure plaque components, including fibrous cap thickness that correlates negatively with $PSS_{peak}$. However, our frame-based analysis was verified in 2mm segments, parameters that segregate different treatments (PA, DC percentage and arc, lumen curvature, irregularity and roughness) are all within VH-IVUS resolution. Lastly, since these studies did not examine MACE, so that our findings are hypothesis-generating, and require further work to determine how high-intensity statins can remodel the lumen/plaque interface.

**CONCLUSION**

We find that changes in $PSS_{peak}$ are associated with complex interactions between plaque architecture, lumen geometry, baseline disease severity and treatment. PSS increased over time in advanced lesions in patients receiving standard medical treatment, but not with high-intensity statins, associated with remodelling artery geometry and plaque architecture. Smoothing plaques and reducing lumen curvature represent novel mechanisms whereby high-intensity statins may protect against plaque rupture.

**Lead author biography**

Professor Martin R. Bennett holds the British Heart Foundation (BHF) Chair of Cardiovascular Sciences at the University of Cambridge, directs the BHF Cambridge Centre for Cardiovascular Research Excellence, and holds Honorary Consultant Cardiologist positions at Cambridge University and Royal Papworth Hospitals. His clinical research programme combines clinical medicine, coronary imaging and engineering for vulnerable plaque detection.

**Supplementary material**

Supplementary material is available at *European Heart Journal Open* online.

**Funding**

This work was funded by British Heart Foundation (BHF) grants FS/19/66/34658, PG/16/24/32090, RG71070, RG84554, the National Institute of Health Research Cambridge Biomedical Research Centre, and the BHF Centre for Research Excellence.

**Conflicts of interest**: none declared.

**Data availability**

The data underlying this article will be shared on reasonable request to the corresponding author.

## References


1. Sabatine MS, Giugliano RP, Keech AC, Honarpour N, Wiviott SD, Murphy SA, Kuder JF, Wang H, Liu T, Wasserman SM, Sever PS, and Pedersen TR, for the FOURIER Steering Committee and Investigators. Evolocumab and clinical outcomes in patients with cardiovascular disease. *N Engl J Med* 2017;**376**:1713–1722.
2. Schwartz GG, Steg PG, Szarek M, Bhatt DL, Bittner VA, Diaz R, Edelberg JM, Goodman SG, Hanotin C, Harrington RA, Jukema JW, Lecorps G, Mahaffey KW, Moryusef A, Pordy R, Quintero K, Roe MT, Sasiela WJ, Tamby JF, Tricoci P, White HD, and Zeiher AM, for the ODYSSEY OUTCOMES Committees and Investigators. Alirocumab and cardiovascular outcomes after acute coronary syndrome. *N Engl J Med* 2018;**379**:2097–2107.
3. Rioufol G, Gilard M, Finet G, Ginon I, Boschat J, André-Fouët X. Evolution of spontaneous atherosclerotic plaque rupture with medical therapy: Long-term follow-up with intravascular ultrasound. *Circulation* 2004;**110**:2875–2880.
4. Stone GW, Maehara A, Lansky AJ, Bruyne B De, Cristea E, Mintz GS, Mehran R, McPherson J, Farhat N, Marso SP, Parise H, Templin B, White R, Zhang Z, Serruys PW. A prospective natural-history study of coronary atherosclerosis. *N Engl J Med* 2011;**364**:226–235.
5. Calvert PA, Obaid DR, O'Sullivan M, Shapiro LM, McNab D, Densem CG, Schofield PM, Braganza D, Clarke SC, Ray KK, West NEJ, Bennett MR. Association between IVUS findings and adverse outcomes in patients with coronary artery disease: The VIVA (VH-IVUS in vulnerable atherosclerosis) study. *JACC Cardiovasc Imaging* Elsevier Inc.; 2011;**4**:894–901.
6. Collins R, Reith C, Emberson J, Armitage J, Baigent C, Blackwell L, Blumenthal R, Danesh J, Smith GD, DeMets D, Evans S, Law M, MacMahon S, Martin S, Neal B,

Poulter N, Preiss D, Ridker P, Roberts I, Rodgers A, Sandercock P, Schulz K, Sever P, Simes J, Smeeth L, Wald N, Yusuf S, Peto R. Interpretation of the evidence for the efficacy and safety of statin therapy. *Lancet* Elsevier Ltd; 2016;**388**:2532–2561.

7. Nissen SE, Nicholls SJ, Sipahi I, Libby P, Raichlen JS, Ballantyne CM, Davignon J, Erbel R, Fruchart JC, Tardif J-C, Schoenhagen P, Crowe T, Cain V, Wolski K, Goormastic M, Tuzcu EM, ASTEROID Investigators  for the. Effect of Very High-Intensity Statin Therapy on Regression of Coronary Atherosclerosis. *JAMA* 2006;**295**:1556.

8. Ballantyne CM, Raichlen JS, Nicholls SJ, Erbel R, Tardif JC, Brener SJ, Cain VA, Nissen SE. Effect of rosuvastatin therapy on coronary artery stenoses assessed by quantitative coronary angiography: A study to evaluate the effect of rosuvastatin on intravascular ultrasound-derived coronary atheroma burden. *Circulation* 2008;**117**:2458–2466.

9. Nicholls SJ, Puri R, Anderson T, Ballantyne CM, Cho L, Kastelein JJP, Koenig W, Somaratne R, Kassahun H, Yang J, Wasserman SM, Scott R, Ungi I, Podolec J, Ophuis AO, Cornel JH, Borgman M, Brennan DM, Nissen SE. Effect of evolocumab on progression of coronary disease in statin-treated patients: The GLAGOV randomized clinical trial. *JAMA - J Am Med Assoc* 2016;**316**:2373–2384.

10. Banach M, Serban C, Sahebkar A, Mikhailidis DP, Ursoniu S, Ray KK, Rysz J, Toth PP, Muntner P, Mosteoru S, García-García HM, Hovingh GK, Kastelein JJP, Serruys PW. Impact of statin therapy on coronary plaque composition: A systematic review and meta-analysis of virtual histology intravascular ultrasound studies. *BMC Med* BMC Medicine; 2015;**13**.

11. Zheng G, Li Y, Huang H, Wang J, Hirayama A, Lin J. The effect of statin therapy on coronary plaque composition using virtual histology intravascular ultrasound: A meta-

analysis. *PLoS One* 2015;**10**:1–14.

12. Nicholls SJ, Puri R, Anderson T, Ballantyne CM, Cho L, Kastelein JJP, Koenig W, Somaratne R, Kassahun H, Yang J, Wasserman SM, Honda S, Shishikura D, Scherer DJ, Borgman M, Brennan DM, Wolski K, Nissen SE. Effect of Evolocumab on Coronary Plaque Composition. *J Am Coll Cardiol* 2018;**72**:2012–2021.
13. Brown AJ, Teng Z, Evans PC, Gillard JH, Samady H, Bennett MR. Role of biomechanical forces in the natural history of coronary atherosclerosis. *Nat Rev Cardiol* 2016;**13**:210–220.
14. Teng Z, Brown AJ, Calvert PA, Parker RA, Obaid DR, Huang Y, Hoole SP, West NEJ, Gillard JH, Bennett MR. Coronary plaque structural stress is associated with plaque composition and subtype and higher in acute coronary syndrome: The BEACON i (Biomechanical Evaluation of Atheromatous Coronary Arteries) study. *Circ Cardiovasc Imaging* 2014;**7**:461–470.
15. Costopoulos C, Huang Y, Brown AJ, Calvert PA, Hoole SP, West NEJ, Gillard JH, Teng Z, Bennett MR. Plaque Rupture in Coronary Atherosclerosis Is Associated With Increased Plaque Structural Stress. *JACC Cardiovasc Imaging* 2017;**10**:1472–1483.
16. Brown AJ, Teng Z, Calvert PA, Rajani NK, Hennessy O, Nerlekar N, Obaid DR, Costopoulos C, Huang Y, Hoole SP, Goddard M, West NEJ, Gillard JH, Bennett MR. Plaque Structural Stress Estimations Improve Prediction of Future Major Adverse Cardiovascular Events after Intracoronary Imaging. *Circ Cardiovasc Imaging* 2016;**9**:1–9.
17. Costopoulos C, Maehara A, Huang Y, Brown AJ, Gillard JH, Teng Z, Stone GW, Bennett MR. Heterogeneity of Plaque Structural Stress Is Increased in Plaques Leading to MACE: Insights From the PROSPECT Study. *JACC Cardiovasc Imaging* 2020;**13**:1206–1218.

18. Costopoulos C, Timmins LH, Huang Y, Hung OY, Molony DS, Brown AJ, Davis EL, Teng Z, Gillard JH, Samady H, Bennett MR. Impact of combined plaque structural stress and wall shear stress on coronary plaque progression, regression, and changes in composition. *Eur Heart J* 2019;**40**:1411–1422.

19. Hung OY, Molony D, Corban MT, Rasoul-Arzrumly E, Maynard C, Eshtehardi P, Dhawan S, Timmins LH, Piccinelli M, Ahn SG, Gogas BD, McDaniel MC, Quyyumi AA, Giddens DP, Samady H. Comprehensive assessment of coronary plaque progression with advanced intravascular imaging, physiological measures, and wall shear stress: A pilot double-blinded randomized controlled clinical trial of nebivolol versus atenolol in nonobstructive coronary. *J Am Heart Assoc* 2016;

20. Eshtehardi P, McDaniel MC, Dhawan SS, Binongo JNG, Krishnan SK, Golub L, Corban MT, Raggi P, Quyyumi AA, Samady H. Effect of intensive atorvastatin therapy on coronary atherosclerosis progression, composition, arterial remodeling, and microvascular function. *J Invasive Cardiol* 2012;**24**.

21. Räber L, Taniwaki M, Zaugg S, Kelbãk H, Roffi M, Holmvang L, Noble S, Pedrazzini G, Moschovitis A, Lüscher TF, Matter CM, Serruys PW, Jüni P, Garcia-Garcia HM, Windecker S. Effect of high-intensity statin therapy on atherosclerosis in non-infarct-related coronary arteries (IBIS-4): A serial intravascular ultrasonography study. *Eur Heart J* 2015;**36**:490–500.

22. Teng Z, Degnan AJ, Sadat U, Wang F, Young VE, Graves MJ, Chen S, Gillard JH. Characterization of healing following atherosclerotic carotid plaque rupture in acutely symptomatic patients: an exploratory study using in vivo cardiovascular magnetic resonance. *J Cardiovasc Magn Reson* 2011;**13**:64.

23. Cheng JM, Garcia-Garcia HM, Boer SPM De, Kardys I, Heo JH, Akkerhuis KM, Oemrawsingh RM, Domburg RT Van, Ligthart J, Witberg KT, Regar E, Serruys PW,

Geuns RJ Van, Boersma E. In vivo detection of high-risk coronary plaques by radiofrequency intravascular ultrasound and cardiovascular outcome: Results of the ATHEROREMO-IVUS study. *Eur Heart J* 2014;**35**:639–647.

24. Nicholls SJ, Ballantyne CM, Barter PJ, Chapman MJ, Erbel RM, Libby P, Raichlen JS, Uno K, Borgman M, Wolski K, Nissen SE. Effect of Two Intensive Statin Regimens on Progression of Coronary Disease. *N Engl J Med* Massachusetts Medical Society; 2011;**365**:2078–2087.

25. Imoto K, Hiro T, Fujii T, Murashige A, Fukumoto Y, Hashimoto G, Okamura T, Yamada J, Mori K, Matsuzaki M. Longitudinal Structural Determinants of Atherosclerotic Plaque Vulnerability: A Computational Analysis of Stress Distribution Using Vessel Models and Three-Dimensional Intravascular Ultrasound Imaging. *J Am Coll Cardiol* 2005;**46**:1507–1515.

26. Teng Z, Sadat U, Li Z, Huang X, Zhu C, Young VE, Graves MJ, Gillard JH. Arterial Luminal Curvature and Fibrous-Cap Thickness Affect Critical Stress Conditions Within Atherosclerotic Plaque: An In Vivo MRI-Based 2D Finite-Element Study. *Ann Biomed Eng* 2010;**38**:3096–3101.

27. Wolfrum S, Jensen KS, Liao JK. Endothelium-Dependent Effects of Statins. *Arterioscler Thromb Vasc Biol* American Heart Association; 2003;**23**:729–736.

28. Joseph L. Nitric Oxide Insufficiency, Platelet Activation, and Arterial Thrombosis. *Circ Res* American Heart Association; 2001;**88**:756–762.

29. Dimmeler S, Zeiher AM. Nitric oxide–an endothelial cell survival factor. *Cell Death Differ* 1999;**6**:964–968.

## Figure Legends

**Figure 1. Study workflow and co-registration of baseline and follow-up VH-IVUS images and corresponding PSS band plots.**

**(A)** Flow chart of study workflow**. (B)** Longitudinal view of VH-IVUS pullback with 5 marked points. The segment of interest was defined using the most proximal and distal side branches (marked with *) seen at baseline **(C)** and follow-up (1, 5) **(D).** Other side branches (2, 3) or fiduciary marks were used to identify corresponding frames, and an interpolation technique applied to find corresponding frames in segments with no landmarks (4). **(E)** Examples of peak and mean plaque structural stress ($PSS_{peak}$ and $PSS_{mean}$) band plots for marked points 2 and 3 at baseline and follow-up.

**Figure 2. Changes in peak and mean PSS with baseline plaque burden after control or high-intensity statin treatment.**

**(A-B)** Change in $PSS_{peak}$ **(A)** or $PSS_{mean}$ **(B)** in all plaques or with different plaque burden in control patients or treated with high-intensity statins. Data are mean (SE), using mixed-effects models. **(C-D)** Interaction plots of linear mixed-effects models showing significant interaction effect of treatment group and baseline plaque burden **(C)** or plaque area **(D)** on $\Delta PSS_{peak}$. PB=plaque burden, PSS=plaque structural stress.

**Figure 3. Changes in plaque geometric parameters or plaque constituents after control or high-intensity statin treatment.**

**(A-C)** Change in **(A)** plaque geometric parameters including external elastic membrane (EEM) area, plaque area and plaque burden, **(B)** necrotic core (NC) area and % or dense calcium (DC) area and %, **(C)** Fibrofatty (FF) area and % or fibrous tissue (FT) area and % in control or high-intensity statin-treated patients. Data are mean (SE) between baseline and follow-up using mixed-effects models.

**Figure 4. Changes in plaque geometric parameters or constituents in advanced lesions (PB>60%) after control or high-intensity statin treatment.**

**(A-C)** Changes in anatomical parameters including external elastic membrane (EEM) area, plaque area and plaque burden **(A)**, necrotic core (NC) area and percentage and dense calcium (DC) area and percentage **(B)**, and fibrofatty (FF) area and percentage and fibrous tissue (FT) area and percentage **(C)** in control patients or after high-intensity statin treatment. Data are mean (SE) using mixed-effects models, n=1,112 frames, total 30 patients.

**Figure 5. Lumen parameter analysis in plaques with baseline PB>60%**

**(A-C)** Linear regression correlation curves for change in peak and mean PSS, with change in **(A)** maximum lumen curvature, **(B)** lumen irregularity, **(C)** lumen roughness, in all plaques with baseline PB>60%. **(D)** Change in lumen curvature, irregularity, roughness and lumen aspect ratio in control patients or after high-intensity statin treatment. Data are mean (SE) by plaque-level mixed effect models, total frames=1,112, plaques=42.

**Figure 6. Examples of changes in PSS due to changes in lumen curvature, irregularity, roughness, and plaque architecture.**

**(A)** Increased $PSS_{peak}$ due to changes in curvature, and calcification/fibrous tissue arrangement. **(B)** Marked increase in $PSS_{peak}$ due to increase in lumen curvature, irregularity and roughness. **(C)** Reduced $PSS_{peak}$ due to changes in curvature, irregularity/roughness, and more confluent calcification. DC=dense calcium; NC=necrotic core; PA=plaque area; PB=plaque burden; $PSS_{peak}$=peak plaque structural stress.

# Tables

**Table 1. Multivariable analysis to assess interaction between baseline plaque burden and treatment group on $\Delta PSS_{peak}$**

| Fixed-effect parameter | **Estimate** | **Standard error** | **P value** |
|---|---|---|---|
| Interaction: Atorvastatin x baseline plaque burden | -1.37 | 0.23 | **<0.0001** |
| Interaction: Rosuvastatin x baseline plaque burden | -1.01 | 0.19 | **<0.0001** |
| Age, as continuous variable | - | - | 0.47 |
| Gender, female vs. male | - | - | 0.78 |
| Hypertension | - | - | 0.64 |
| Current smoker | - | - | 0.065 |
| Diabetes | - | - | 0.16 |
| Family history of CAD | - | - | 0.70 |
| Prior statin use | - | - | 0.25 |

CAD, coronary artery disease; PSS, plaque structural stress.

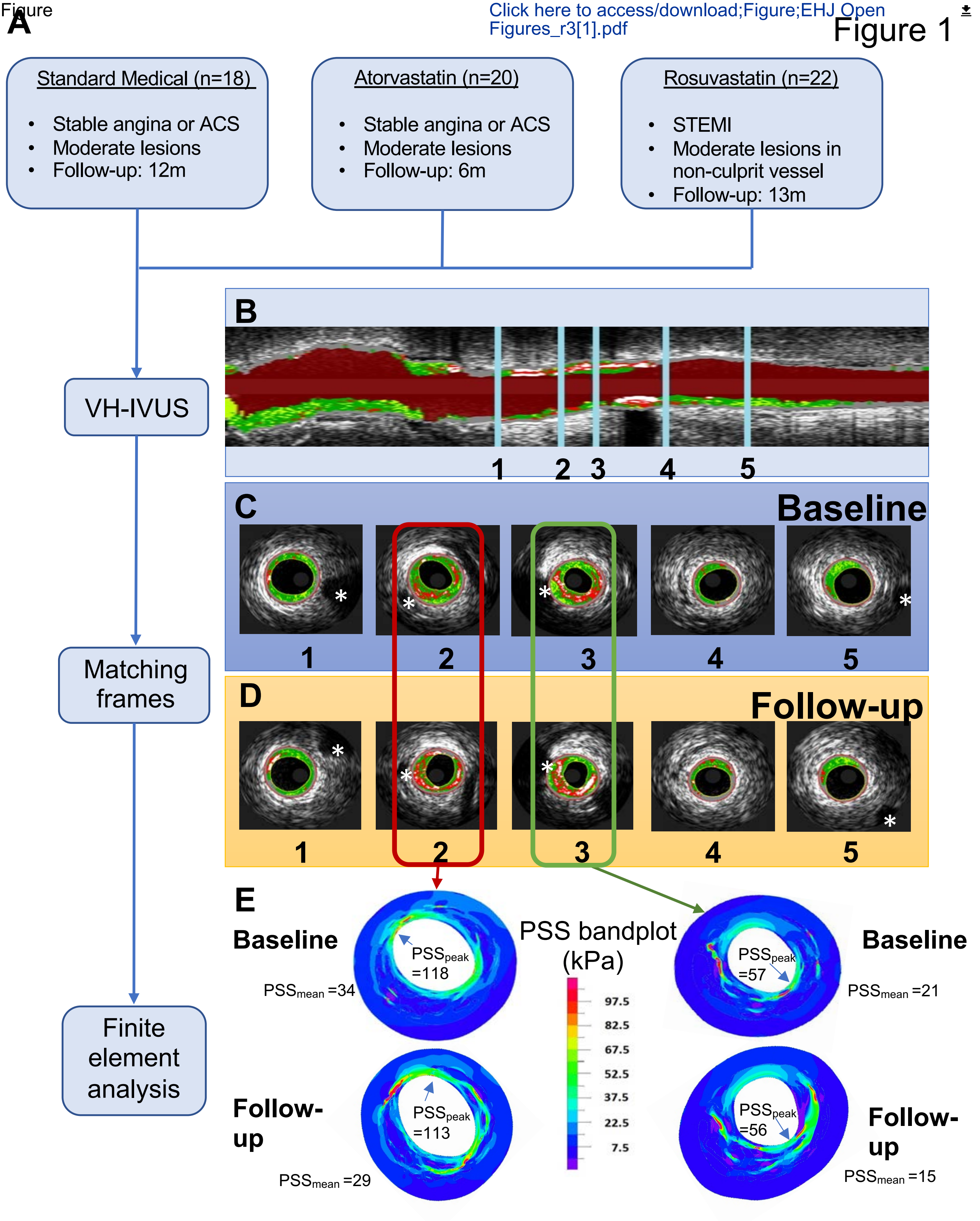


**Figure 1. Study workflow and co-registration of baseline and follow-up VH-IVUS images and corresponding PSS band plots.**
**(A)** Flow chart of study workflow. **(B)** Longitudinal view of VH-IVUS pullback with 5 marked points. The segment of interest was defined using the most proximal and distal side branches (marked with *) seen at baseline **(C)** and follow-up (1, 5) **(D)**. Other side branches (2, 3) or fiduciary marks were used to identify corresponding frames, and an interpolation technique applied to find corresponding frames in segments with no landmarks (4). **(E)** Examples of peak and mean plaque structural stress ($PSS_{peak}$ and $PSS_{mean}$) band plots for marked points 2 and 3 at baseline and follow-up.

Figure 2

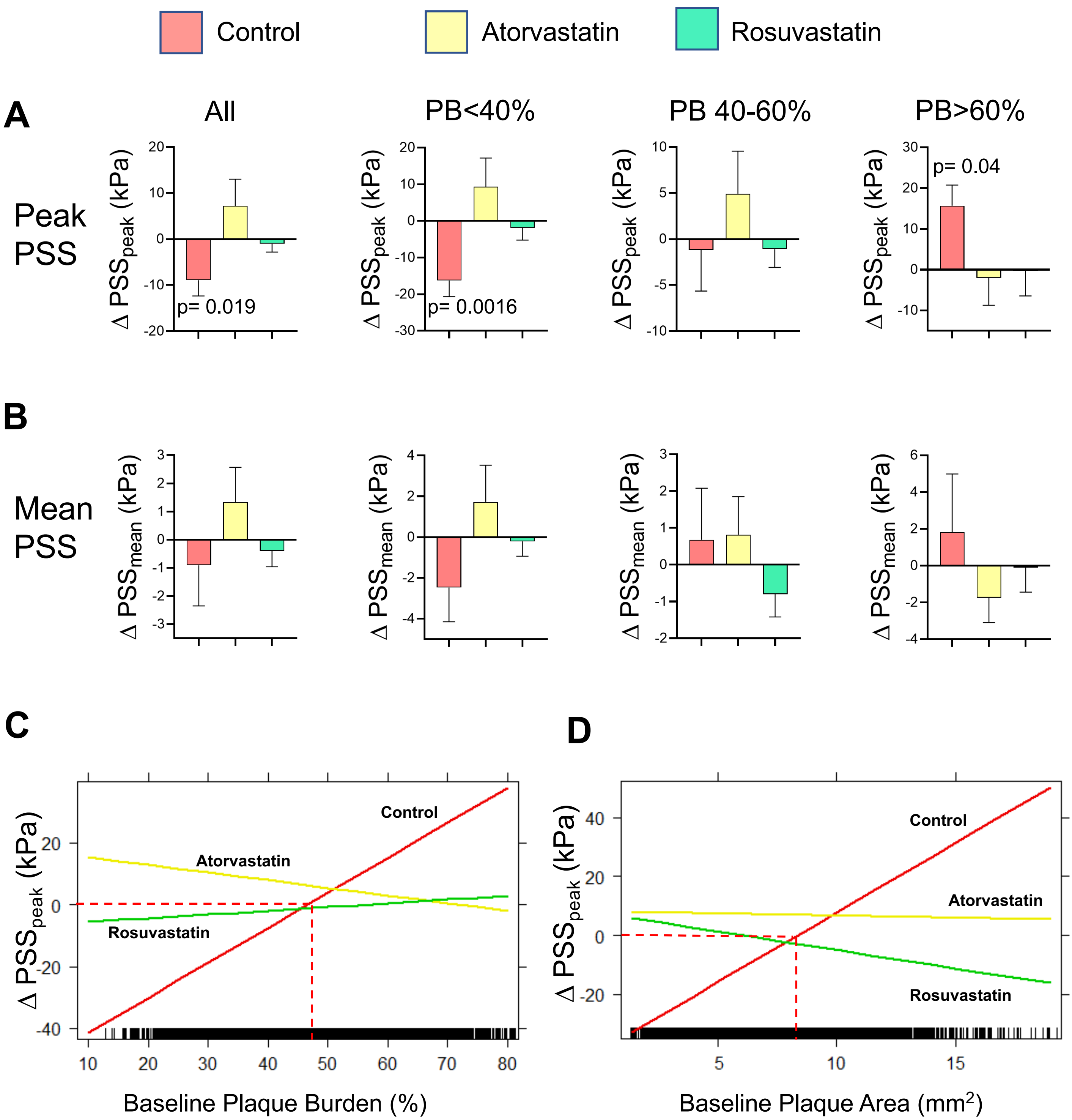


**Figure 2. Changes in peak and mean PSS with baseline plaque burden after control or high-intensity statin treatment.**
**(A-B)** Change in PSS$_{peak}$ **(A)** or PSS$_{mean}$ **(B)** in all plaques or with different plaque burden in control patients or treated with high-intensity statins. Data are mean (SE), using mixed-effects models. **(C-D)** Interaction plots of linear mixed-effects models showing significant interaction effect of treatment group and baseline plaque burden **(C)** or plaque area **(D)** on ΔPSS$_{peak}$. PB=plaque burden, PSS=plaque structural stress.

Figure 3

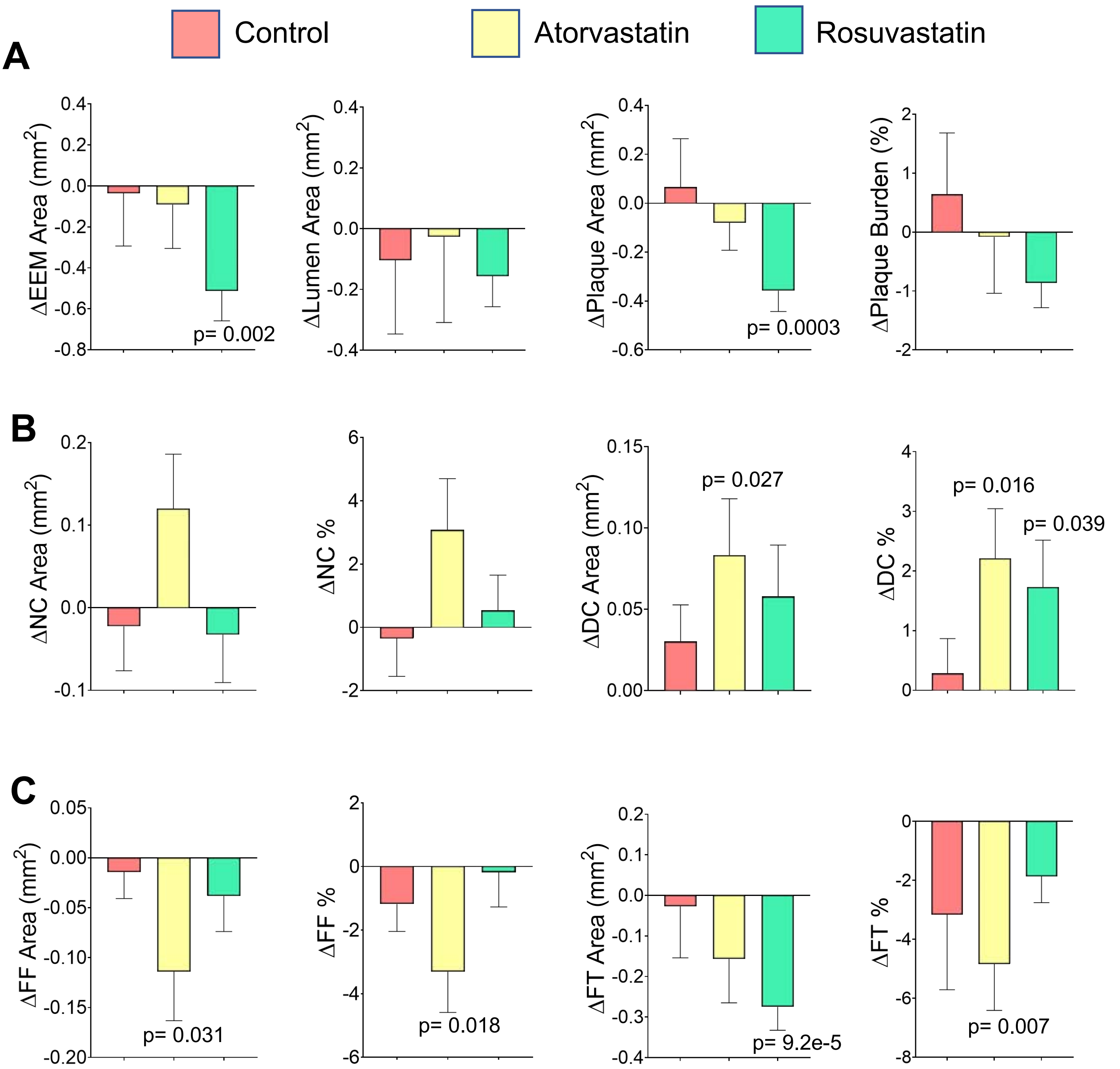


**Figure 3. Changes in plaque geometric parameters or plaque constituents after control or high-intensity statin treatment.**

**(A-C)** Change in **(A)** plaque geometric parameters including external elastic membrane (EEM) area, plaque area and plaque burden, **(B)** necrotic core (NC) area and % or dense calcium (DC) area and %, **(C)** Fibrofatty (FF) area and % or fibrous tissue (FT) area and % in control or high-intensity statin-treated patients. Data are mean (SE) between baseline and follow-up using mixed-effects models.

Figure 4

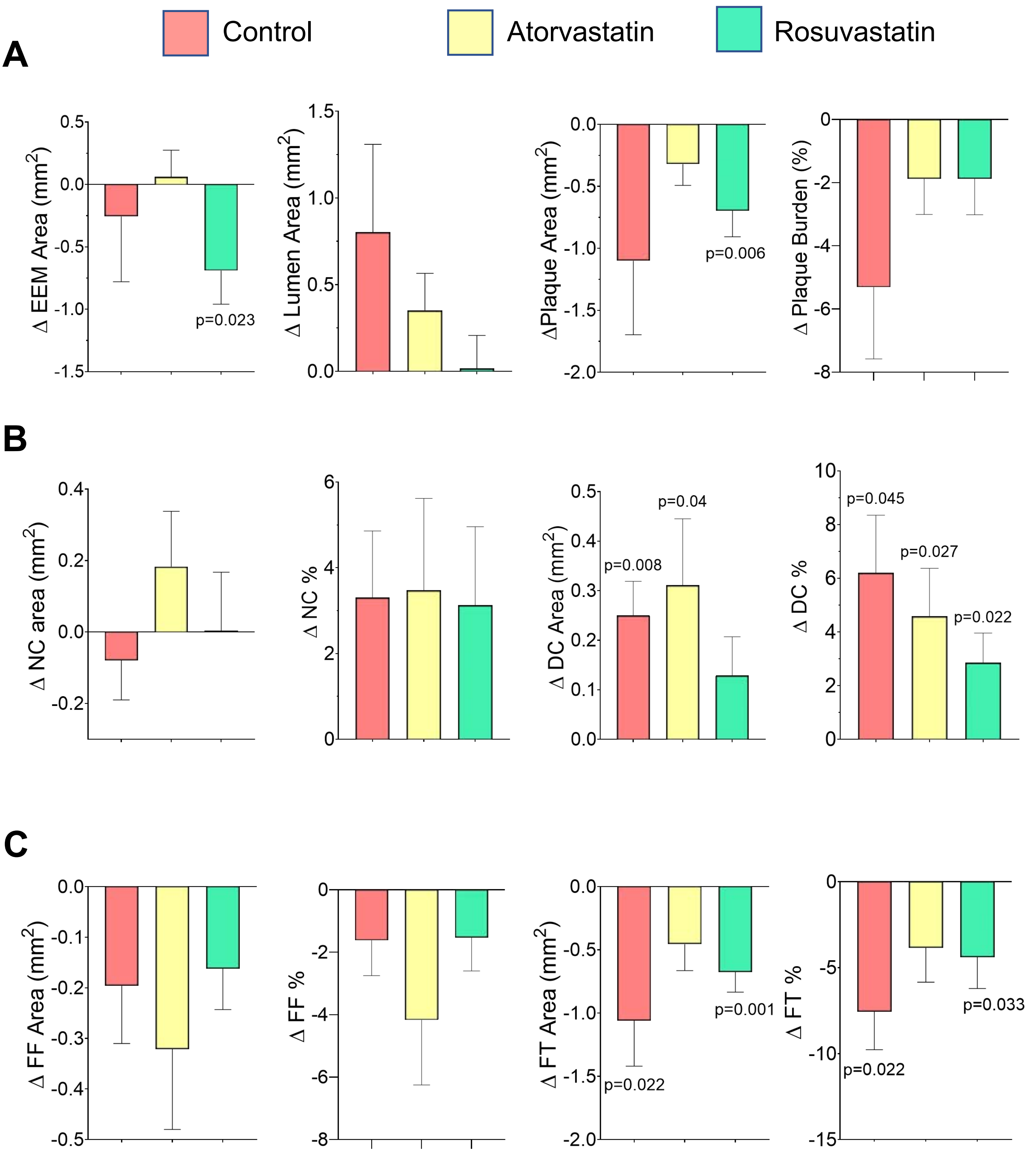


**Figure 4. Changes in plaque geometric parameters or constituents in advanced lesions (PB>60%) after control or high-intensity statin treatment.**

**(A-C)** Changes in anatomical parameters including external elastic membrane (EEM) area, plaque area and plaque burden **(A)**, necrotic core (NC) area and percentage and dense calcium (DC) area and percentage **(B)**, and fibrofatty (FF) area and percentage and fibrous tissue (FT) area and percentage **(C)** in control patients or after high-intensity statin treatment. Data are mean (SE) using mixed-effects models, n=1,112 frames, total 30 patients.

Figure 5

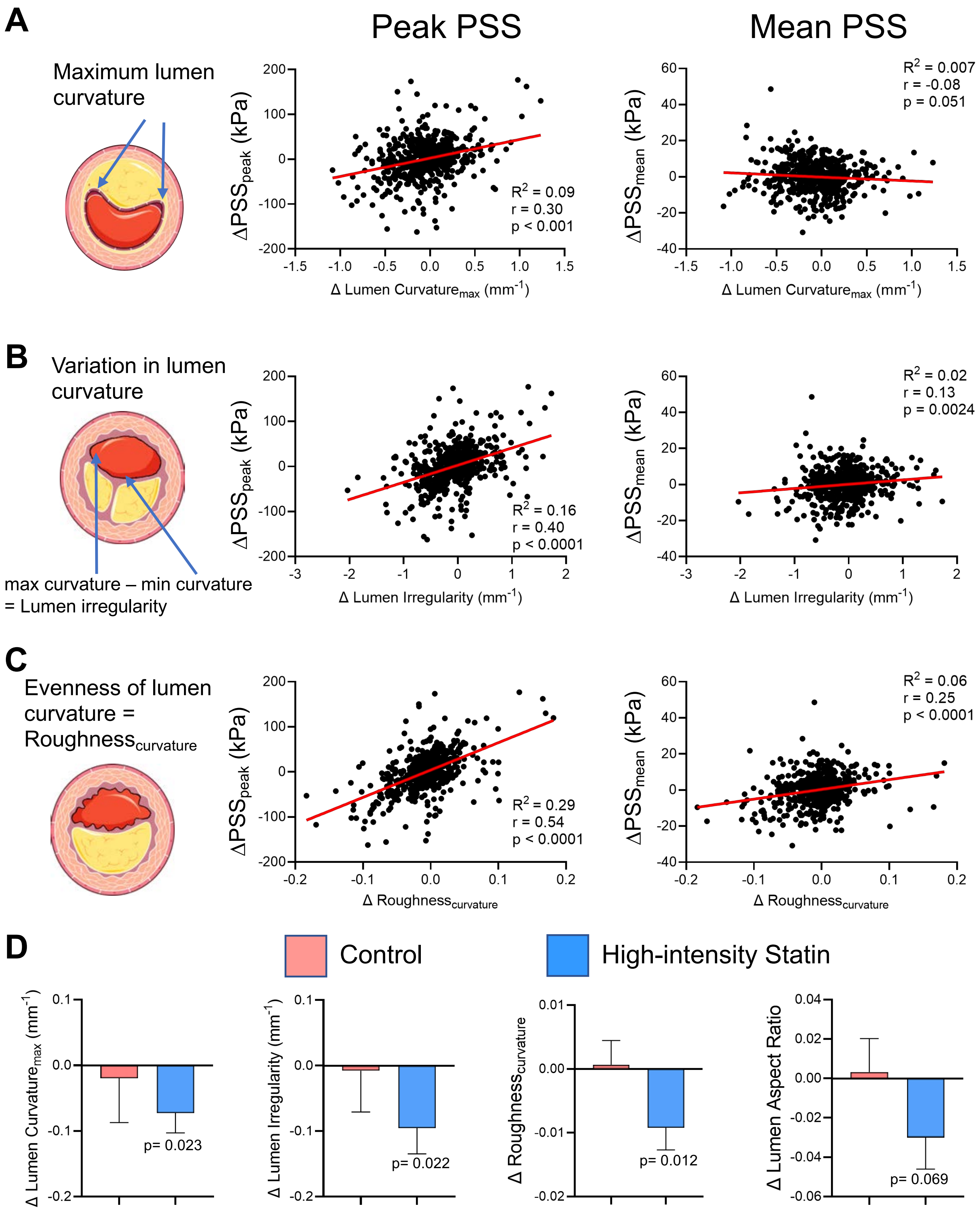


**Figure 5. Lumen parameter analysis in plaques with baseline PB>60%**
**(A-C)** Linear regression correlation curves for change in peak and mean PSS, with change in **(A)** maximum lumen curvature, **(B)** lumen irregularity, **(C)** lumen roughness, in all plaques with baseline PB>60%. **(D)** Change in lumen curvature, irregularity, roughness and lumen aspect ratio in control patients or after high-intensity statin treatment. Data are mean (SE) by plaque-level mixed effect models, total frames=1,112, plaques=42.

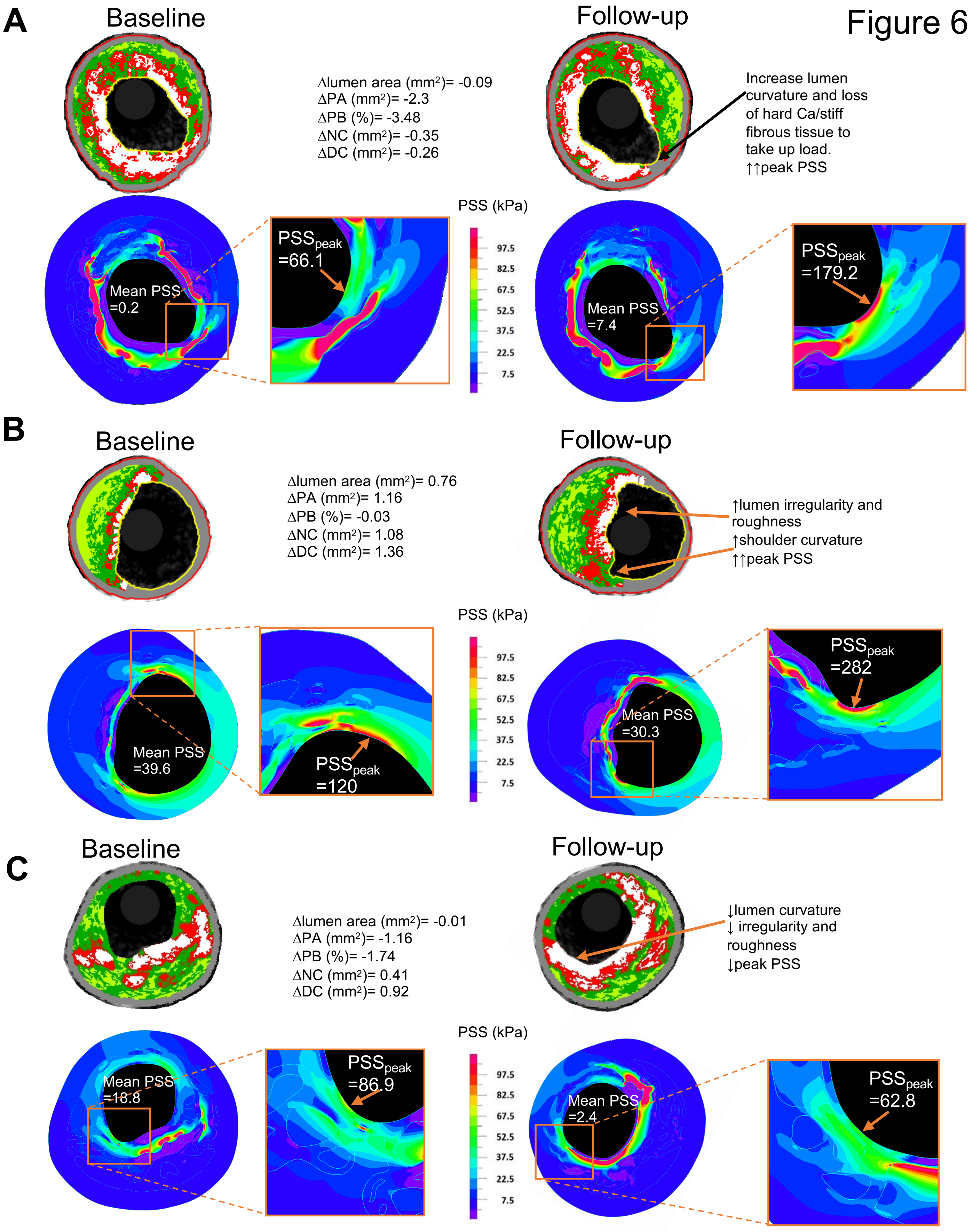


**Figure 6. Examples of changes in PSS due to changes in lumen curvature, irregularity, roughness, and plaque architecture.**

**(A)** Increased $PSS_{peak}$ due to changes in curvature, and calcification/fibrous tissue arrangement. **(B)** Marked increase in $PSS_{peak}$ due to increase in lumen curvature, irregularity and roughness. **(C)** Reduced $PSS_{peak}$ due to changes in curvature, irregularity/roughness, and more confluent calcification. DC=dense calcium; NC=necrotic core; PA=plaque area; PB=plaque burden; $PSS_{peak}$=peak plaque structural stress.

# SUPPLEMENTAL MATERIAL

## Supplemental Methods

### Biomechanical modeling of plaque structural stress

Plaque geometry was constructed from VH-IVUS images using an in-house developed MATLAB code (proprietary code, MATLAB R2020a, MathWorks, Inc, Natick, Massachusetts, USA). Each VH-IVUS frame was segmented into its individual components, and a 5% circumferential shrinkage applied to generate a zero-pressure condition as *in vivo* data were recorded during diastole. A 65µm layer of fibrous tissue was introduced during mesh generation to account for the limited axial resolution of VH-IVUS to detect a fibrous cap. The vessel wall and all plaque components were assumed to be hyper-elastic, non-linear, isotropic, incompressible, and piecewise homogeneous. The modified Mooney-Rivlin model was used to describe the material property of each component:

$$W = c_1(\bar{I}_1 - 3) + D_1\left[e^{D_2(\bar{I}_1 - 3)} - 1\right] + \kappa(J - 1)$$

where $\bar{I}_1 = J^{-2/3}I_1$ with $I_1$ being the first strain invariant of the unimodular component of the left Cauchy-Green deformation tensor. $J = det(\boldsymbol{F})$ and $\boldsymbol{F}$ is the deformation gradient. $\kappa$ is the Lagrangian multiplier for the incompressibility. $c_1$, $D_1$ and $D_2$ are material parameters derived from direct material testing results. In this study, the following values were used: arterial wall, $c_1$=0.14 kPa, $D_1$=3.83 kPa, $D_2$=18.80 kPa; fibrous tissue, $c_1$=0.19 kPa, $D_1$=5.77 kPa, $D_2$=18.22 kPa; necrotic core, $c_1$=0.05 kPa, $D_1$=4.89 kPa, $D_2$=5.43 kPa and dense calcification, $c_1$=1.15x$10^5$ kPa, $D_1$=7.67x$10^4$ kPa, $D_2$=2.84x$10^{-8}$ kPa.[1,2] The motion of each atherosclerotic component is governed by kinetic equations as:

$$\rho v_{i,tt} = \sigma_{ij,j} \; (i, j = 1, 2)$$

where $[v_i]$ and $[\sigma_{ij}]$ are the displacement vector and stress tensor, respectively, $\rho$ is the density of each component, and $t$ is time.

The entire plaque geometric model was meshed using 9-node quadrilaterals, generating approximately 10,000 elements and 40,000 nodes per model. Displacement and strain were assumed to be large. There was no relative movement at the interface of atherosclerotic components and the relative energy tolerance was set to be 0.005. Two adjacent points located on the outer wall were fixed to prevent rigid body displacement. Maximum principal stress was used to characterize the mechanical loading within the plaque structure (PSS) in the peri-luminal region (0.2mm maximum depth from the luminal contour). Mean PSS was calculated as the mean value of PSS experienced by all the luminal nodes. Dynamic loading conditions were standardized to 120/70mmHg. Pressure at the outer boundary was set to zero. All simulations were performed using ADINA 9.5 (ADINA R&D, Inc., USA) software.

**Additional measures (*Figure S1*):**

- **Lumen aspect ratio** = maximum diameter of ellipse (or lumen major axis)/minimum diameter of ellipse (or lumen minor axis), i.e., lower (improved) aspect ratio describes a rounder lumen, and a value of 1 indicates a perfectly circular lumen.
- **Lumen curvature:**[3,4] curvature at point a (in ***Figure S1***) was computed using the radius (as $r_a$) of the circle determined by point a and two adjacent points (bottom right figure) on both sides, i.e. curvature = $1/r_a$. Curvature value was computed for all points in the lumen, and the maximum lumen curvature value (Lumen $\text{Curvature}_{max}$) is used in data analysis. The minimum lumen curvature value (Lumen $\text{Curvature}_{min}$) is also computed for lumen irregularity calculation

- **Lumen irregularity**[5] = Lumen Curvature$_{max}$ – Lumen Curvature$_{min}$
- **Lumen roughness:** reflects the lumen surface evenness in respect to curvature, and calculated using the following formula, with smaller values representing more round or even surface and a perfect round lumen shape will have roughness being 1. Method adapted from.[6]

$$Roughness_{Curvature} = \sqrt{\frac{1}{2\pi r} \sum \left(\frac{r}{r_a}\right)^2 \Delta l}$$

(r is the radius of the circle best fitting the lumen contour; $r_a$ is defined as above in lumen curvature calculation; and Δl is the length between point a and one adjacent point.)

**Assessment of analyst variability**

The reproducibility of matching between baseline and follow-up VH-IVUS frames by 2 analysts was examined in 6 vessels that had both baseline (n= 573 frames) and follow-up (n= 623 frames). The 2 analysts reviewed the VH-IVUS data and separately identified the location of follow-up frames in the 2mm segments defined in the baseline frames. To report the intra-observer variability the 1st analyst performed the analysis twice. The κ test of concordance was used to assess agreement. A good overall agreement was noted for the estimation of the two analysts with the intra-observer variability being 0.733 and the inter-observer variability being 0.701. The reproducibility of lumen curvature, irregularity, and roughness assessment was examined on 2 randomly selected vessels (77 frames) by testing the intraclass correlation coefficient (ICC); this achieved good to excellent absolute agreement: lumen curvature, ICC= 0.787; lumen irregularity, ICC = 0.72; lumen roughness, ICC= 0.712.

**Statistical analysis of patient demographics**

Continuous variables are presented as mean ± standard deviation or median (interquartile range) and discrete variables as absolute numbers (percentage). Normality tests were performed for all variables using quantile-quantile plots, and Kolmogorox-Smirnov/Shapiro-Wilks test where appropriate. Student's t-test or one-way ANOVA were used for normally distributed continuous variables. Non-normally distributed variables were analyzed using Mann-Whitney U test or Kruskal-Wallis test for independent samples, and Wilcoxon signed-rank test for paired samples. Chi-square test ($\chi^2$) or Fisher's exact test was used for discrete variables where appropriate. We identified a number of potential clinically important confounding factors (age as continuous variable, gender, hypertension, smoking status, diabetes, family history of coronary artery disease, and prior statin use), and these were added in the multivariable model as fixed effects to examine our main study finding.

## Supplemental Tables

### Table S1. Trial groups, inclusion and exclusion criteria

| | Control | Atorvastatin | Rosuvastatin |
|---|---|---|---|
| Treatment | Aspirin, low-intensity statin, β-blocker | Atorvastatin 80mg | Rosuvastatin 40mg |
| Trial registration | NCT01230892 | NCT00576576 | NCT00962416 |
| Patient number | n= 18 | n= 20 | n= 22 |
| Follow-up period | 12 months | 6 months | 13 months |
| **Inclusion criteria** | | | |
| Presentation | Stable angina or NSTEMI | Stable angina or ACS | STEMI |
| Age | 21 to 79 years | ≥ 18 years | 18 to 89 years |
| Lesion | Moderate lesions requiring physiologic assessment<br>On stable medical therapy | Moderate lesions requiring invasive physiologic evaluation | 2 major proximal arteries suitable for intracoronary imaging |
| **Exclusion criteria** | | | |
| Hemodynamic | STEMI<br>Cardiogenic shock | STEMI, cardiogenic shock, hemodynamic instability | Acute MI due to stent thrombosis<br>Mechanical complication of acute MI |
| Lesion specific | Lesions requiring revascularization<br>LM>50% stenosis<br>Lesion beyond 60mm<br>Significant visual collaterals | Lesions requiring PCI or CABG<br>LM >50% stenosis<br>Lesion beyond 60mm<br>Visual collaterals | Lesions requiring treatment (stenosis>50%) in 2 major proximal arteries<br>Infarct lesion at site of a previously implanted stent |
| Other cardiac history | CABG<br>Severe valvular heart disease<br>EF<30% | CABG<br>severe valvular heart disease | - |
| Treatment | Contraindication to β-blockers, CCBs or extended-release nitrate therapy within last 48 hours | On maximum dose of statin<br>On statin with an LDL≤130mg/dl | Known intolerance to aspirin, clopidogrel, heparin, stainless steel, biolimus or contrast material |
| Other comorbidities | Creatinine>1.5mg/dL, renal impairment<br>Liver impairment | Creatinine>1.5mg/dL<br>Liver disease<br>Uncontrolled diabetes<br>Uncontrolled hypertension | Renal failure<br>Planned surgery within 6 months of PCI<br>Life expectancy <1 year |
| Pregnancy | - | Pregnancy or planned pregnancy | Female of childbearing potential |
| Coagulopathy | Hematologic disease | INR>1.8<br>Hematologic disease | Bleeding diathesis/known coagulopathy<br>Use of warfarin |
| Other trial | - | - | Currently participating in another trial before reaching first endpoint |

ACS, acute coronary syndrome; CABG, coronary artery bypass graft; CCB, calcium channel blocker; EF, ejection fraction; INR, international normalized ratio; LDL, low-density lipoproteins; LM, left main stem artery; MACE, major adverse cardiac events; MI, myocardial infarction; NSTEMI, non-ST elevation myocardial infarction; PCI, percutaneous coronary intervention; STEMI, ST-segment elevation myocardial infarction

## Table S2. Patient demographic and clinical characteristics

| | Control (C) n=18 | Atorvastatin (A) n=20 | Rosuvastatin (R) n=22 | P value | | |
|---|---|---|---|---|---|---|
| | | | | C vs. A | C vs. R | A vs. R |
| Age, years (mean ± SD) | 51.0 ±10.2 | 55.9 ± 12.5 | 57.6 ± 9.7 | 0.36 | 0.14 | 0.855 |
| Male, n (%) | 8 (44.4) | 13 (65) | 20 (90.9) | 0.203 | **0.002** | 0.062 |
| BMI, kg/m$^2$ (mean ± SD) | 29.2 ± 5.8 | 31.9 ± 5.9 | 27.2 ± 3.8 | 0.259 | 0.451 | **0.014** |
| Hypertension, n (%) | 12 (66.7) | 14 (70) | 11 (50) | 0.825 | 0.289 | 0.187 |
| Current smoking, n (%) | 1 (5.6) | 5 (25) | 11 (50) | 0.184 | **0.004** | 0.096 |
| Diabetes, n (%) | 3 (16.7) | 6 (30) | 2 (9.1) | 0.454 | 0.642 | 0.123 |
| Hypercholesterolemia n (%) | 12 (66.7) | 17 (85) | 8 (36.4) | 0.26 | 0.057 | **0.002** |
| Family history of CAD, n (%) | 8 (44.4) | 7 (35) | 5 (22.7) | 0.552 | 0.145 | 0.379 |
| Previous MI, n (%) | 4 (22.2) | 2 (10) | 1 (4.5) | 0.395 | 0.155 | 0.598 |
| Previous PCI | 5 (27.8) | 4 (20) | 1 (4.5) | 0.709 | 0.073 | 0.174 |
| **Presentation** | | | | | | |
| Stable angina, n (%) | 13 (72.2) | 13 (65) | 0 | 0.632 | - | - |
| ACS, n (%) | 5 (27.8) | 7 (35) | 0 | 0.632 | - | - |
| STEMI, n (%) | 0 (0) | 0 (0) | 22 (100) | - | - | - |
| **Prior Medications** | | | | | | |
| Statin, n (%) | 12 (66.7) | 4 (20) | 1 (4.5) | **0.008** | **<0.001** | 0.174 |
| β-blockers, n (%) | 7 (38.9) | 8 (40) | 2 (9.1) | 0.944 | 0.053 | **0.03** |
| Aspirin, n (%) | 13 (72.2) | 13 (65) | 1 (4.5) | 0.632 | **<0.001** | **<0.001** |
| Antiplatelet, n (%) | 5 (27.8) | 3 (15) | 0 (0) | 0.438 | **0.013** | 0.099 |
| CCB, n (%) | 5 (27.8) | 2 (10) | 1 (4.5) | 0.222 | 0.073 | 0.598 |
| Nitrate, n (%) | 13 (72.2) | 4 (20) | 0 (0) | **0.003** | **<0.001** | **0.043** |
| ACE inhibitor or ARB, n (%) | 5 (27.8) | 10 (50) | 5 (22.7) | 0.162 | 0.714 | 0.065 |
| **Lipid levels** | | | | | | |
| Change in LDL, mg/dL (mean ± SD) | **17.2 ± 35.8*** | **-47.5 ± 30.5†** | **-29.8 ± 38.2‡** | **<0.001** | **<0.001** | 0.256 |
| Change in HDL, mg/dL (mean ± SD) | 0.4 ± 10.8§ | 1.8 ± 8.5‖ | **5.0 ± 8.4¶** | 0.869 | 0.285 | 0.551 |
| **Blood pressure** | | | | | | |
| Change in mean arterial pressure, mmHg (mean ± SD) | -2.6 ± 15.5 | 0.1 ± 16.3 | -2.7 ± 13.3 | 0.852 | 0.999 | 0.853 |

ACE, angiotensin converting enzyme; ACS, acute coronary syndrome; ARB, angiotensin receptor blocker; BMI, body mass index; CAD, coronary artery disease; CCB, calcium channel blocker; HDL, high-density lipoprotein; LDL, low-density lipoprotein; MI, myocardial infarction; NSTEMI, non-ST segment elevation myocardial infarction; SD, standard deviation; STEMI, ST-segment elevation myocardial infarction; UA, unstable angina.

*p=0.031; † p<0.001; ‡ p=0.003; § p=0.877; || p=0.308; ¶ p=0.014.

**Table S3. Baseline VH-IVUS characteristics**

| Characteristics, mean ± SE | **Control (C) frame n=766 patient=18** | **Atorvastatin (A) frame n=1218 patient=20** | **Rosuvastatin (R) frame n=1690 patient=22** | **P value** | | |
|---|---|---|---|---|---|---|
| | | | | **C vs. A** | **C vs. R** | **R vs. A** |
| EEM area, $mm^2$ | 16.71 ± 0.20 | 16.29 ± 0.14 | 14.18 ± 0.11 | 0.902 | **0.028** | **0.033** |
| Lumen area, $mm^2$ | 10.21 ± 0.15 | 9.11 ± 0.11 | 7.16 ± 0.06 | 0.355 | **0.001** | **0.01** |
| Plaque area, $mm^2$ | 6.50 ± 0.11 | 7.18 ± 0.08 | 7.01 ± 0.07 | 0.304 | 0.663 | 0.515 |
| Plaque burden (%) | 39.6 ± 0.49 | 44.4 ± 0.38 | 48.5 ± 0.29 | 0.122 | **0.003** | 0.156 |
| NC% | 17.7 ± 0.45 | 18.5 ± 0.34 | 20.2 ± 0.32 | 0.823 | 0.327 | 0.421 |
| NC area, $mm^2$ | 0.70 ± 0.03 | 0.80 ± 0.02 | 1.00 ± 0.02 | 0.578 | 0.16 | 0.357 |
| DC% | 6.31 ± 0.33 | 7.40 ± 0.26 | 8.00 ± 0.23 | 0.268 | 0.164 | 0.761 |
| DC area, $mm^2$ | 0.23 ± 0.01 | 0.33 ± 0.01 | 0.41 ± 0.01 | 0.107 | 0.052 | 0.532 |
| FT% | 65.9 ± 0.72 | 64.7 ± 0.48 | 57.9 ± 0.49 | 0.395 | **0.004** | **0.021** |
| FT area, $mm^2$ | 1.92 ± 0.06 | 2.39 ± 0.05 | 2.21 ± 0.03 | 0.258 | 0.592 | 0.441 |
| FF% | 6.90 ± 0.23 | 8.75 ± 0.23 | 9.34 ± 0.23 | 0.093 | 0.198 | 0.667 |
| FF area, $mm^2$ | 0.22 ± 0.01 | 0.39 ± 0.01 | 0.33 ± 0.01 | **0.034** | 0.25 | 0.167 |

Data are mean (SE)

DC, dense calcification; EEM, external elastic membrane; FF, fibrofatty tissue; FT, fibrous tissue; NC, necrotic core; SE, standard error; VH-IVUS, virtual histology intravascular ultrasound

**Table S4. Segmental analysis on changes in peak and mean plaque structural stress with different statin regimes and baseline disease severity**

| | Control | | Atorvastatin | | Rosuvastatin | |
|---|---|---|---|---|---|---|
| **Overall** | Segment=237 | P value | Segment=374 | P value | Segment=445 | P value |
| ΔPeak PSS, kPa (mean ± SE) | -8.6 ± 3.6 | **0.03** | 6.2 ± 5.9 | 0.306 | -1.4 ± 1.8 | 0.446 |
| ΔMean PSS, kPa (mean ± SE) | -1.1 ± 1.5 | 0.481 | 1.2 ± 1.2 | 0.34 | -0.5 ± 0.6 | 0.399 |
| **Baseline PB<40%** | Segment=141 | P value | Segment=165 | P value | Segment=94 | P value |
| ΔPeak PSS, kPa (mean ± SE) | -16.7 ± 5.0 | **0.004** | 9.1 ± 8.0 | 0.272 | -2.9 ± 3.4 | 0.405 |
| ΔMean PSS, kPa (mean ± SE) | -2.4 ± 1.8 | 0.2 | 1.7 ± 1.9 | 0.368 | 0.2 ± 0.8 | 0.82 |
| **Baseline PB=40-60%** | Segment=71 | P value | Segment=168 | P value | Segment=269 | P value |
| ΔPeak PSS, kPa (mean ± SE) | -2.3 ± 4.5 | 0.608 | 6.6 ± 5.2 | 0.224 | -1.2 ± 2.0 | 0.562 |
| ΔMean PSS, kPa (mean ± SE) | -0.7 ± 1.3 | 0.625 | 0.8 ± 1.1 | 0.466 | -1.1 ± 0.6 | 0.076 |
| **Baseline PB>60%** | Segment=25 | P value | Segment=41 | P value | Segment=82 | P value |
| ΔPeak PSS, kPa (mean ± SE) | 19.4 ± 6.1 | 0.058 | -7.2 ± 7.1 | 0.412 | -2.0 ± 5.7 | 0.735 |
| ΔMean PSS, kPa (mean ± SE) | 1.5 ± 3.4 | 0.681 | -0.2 ± 1.9 | 0.936 | -0.2 ± 1.4 | 0.88 |

PB, plaque burden; PSS, plaque structural stress; SE, standard error.

**Table S5. Correlation between changes in peak and mean PSS and plaque geometric and compositional parameters**

| | $\Delta PSS_{peak}$ (kPa) | | | $\Delta PSS_{mean}$ (kPa) | | |
|---|---|---|---|---|---|---|
| | Correlation coefficient (r) | $R^2$ | p | Correlation coefficient (r) | $R^2$ | p |
| ΔLumen area ($mm^2$) | 0.297 | 0.088 | **<0.0001** | 0.584 | 0.34 | **<0.0001** |
| ΔPlaque area ($mm^2$) | -0.16 | 0.026 | **<0.0001** | -0.4 | 0.16 | **<0.0001** |
| ΔPlaque burden (%) | -0.261 | 0.068 | **<0.0001** | -0.6 | 0.36 | **<0.0001** |
| ΔLumen aspect ratio | 0.346 | 0.12 | **<0.0001** | 0.026 | 0.0007 | 0.11 |
| ΔNC area ($mm^2$) | -0.024 | 0.0006 | 0.142 | -0.16 | 0.026 | **<0.0001** |
| ΔNC % | 0.033 | 0.001 | **0.046** | -0.064 | 0.004 | **<0.0001** |
| ΔFF area ($mm^2$) | -0.071 | 0.005 | **<0.0001** | -0.116 | 0.014 | **<0.0001** |
| ΔFF % | -0.0046 | 2.1e-5 | 0.78 | -0.051 | 0.003 | **0.002** |
| ΔFT area ($mm^2$) | -0.151 | 0.023 | **<0.0001** | -0.272 | 0.074 | **<0.0001** |
| ΔFT % | -0.061 | 0.004 | **0.0002** | -0.072 | 0.005 | **<0.0001** |
| ΔDC area ($mm^2$) | -0.01 | 0.0001 | 0.52 | -0.33 | 0.11 | **<0.0001** |
| ΔDC % | 0.05 | 0.0026 | **0.0022** | -0.202 | 0.041 | **<0.0001** |
| ΔMaximum arc of DC (°) | 0.02 | 0.0004 | 0.21 | -0.417 | 0.17 | **<0.0001** |
| ΔTotal arc of DC (°) | -0.013 | 0.0002 | 0.44 | -0.428 | 0.18 | **<0.0001** |

DC, dense calcium; FF, fibrofatty; FT, fibrous tissue; NC, necrotic core; PSS, plaque structural stress.

**Table S6. Peri-MLA analysis on changes in lumen geometric features in plaques with baseline PB>60%**

| Characteristics<br>mean ± SE | Control | | High-intensity statin | |
|---|---|---|---|---|
| | **frame =84** | **p** | **frame =412** | **p** |
| $\Delta$Curvature$_{max}$ ($mm^{-1}$) | -0.070 ± 0.090 | 0.464 | -0.0773 ± 0.0378 | 0.0513 |
| $\Delta$Irregularity ($mm^{-1}$) | -0.113 ± 0.0769 | 0.196 | -0.139 ± 0.0544 | **0.0174** |
| $\Delta$Roughness$_{curvature}$ | -0.00638 ± 0.00816 | 0.462 | -0.0161 ± 0.00583 | **0.0108** |
| $\Delta$Lumen aspect ratio | -0.010 ± 0.024 | 0.678 | -0.059 ± 0.021 | **0.01** |

MLA, minimal luminal area; PB, plaque burden; SE, standard error.

Figure S1

# Supplemental Figures

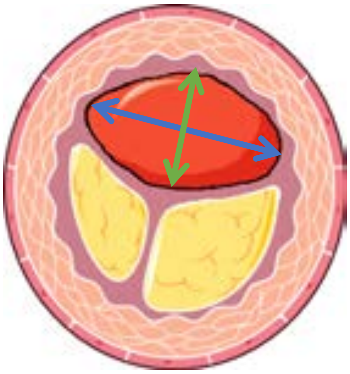

- Lumen aspect ratio = $\dfrac{\textit{lumen major axis}}{\textit{lumen minor axis}}$

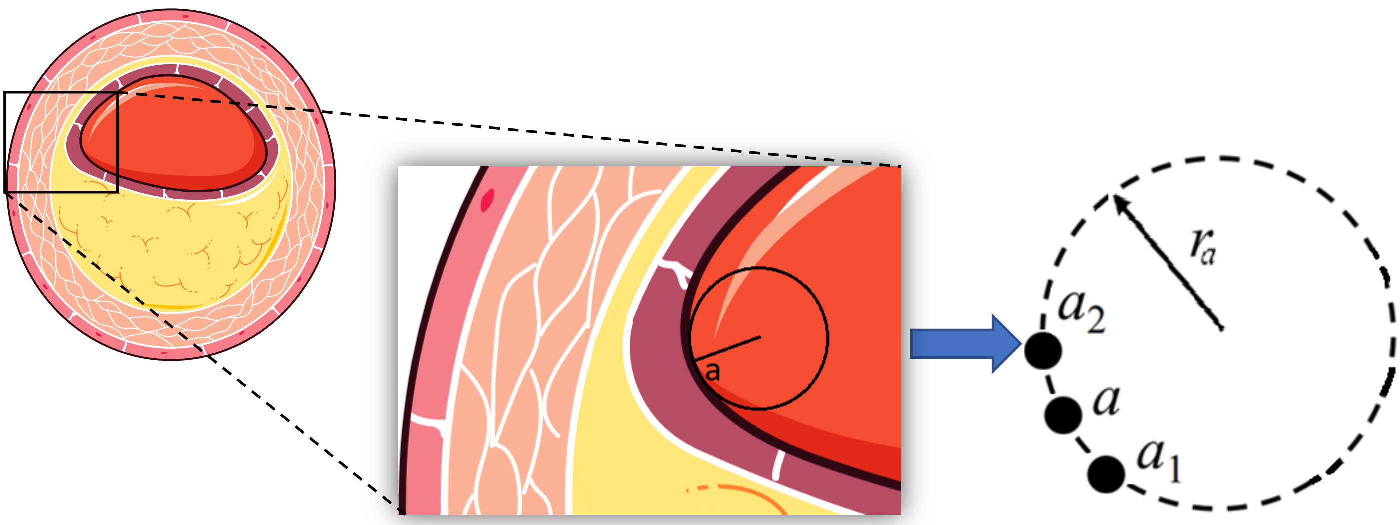


- Lumen curvature: curvature at point a was computed using the radius (as $r_a$) of the circle determined by point a and two adjacent points ($a_1$ and $a_2$), i.e. Lumen Curvature = $1/r_a$.

- Lumen Irregularity= Lumen Curvature$_{max}$ – Lumen Curvature$_{min}$

- $$Roughness_{Curvature} = \sqrt{\frac{1}{2\pi r} \sum \left(\frac{r}{r_a}\right)^2 \Delta l}$$

- Roughness as a measure of evenness of lumen curvature. r is the radius of the circle best fitting the lumen contour (i.e. lumen area =$\pi r^2$), $\Delta l$ is the length between point a and one adjacent point

**Figure S1. Definitions of lumen aspect ratio, curvature, irregularity, and roughness**

Figure S2

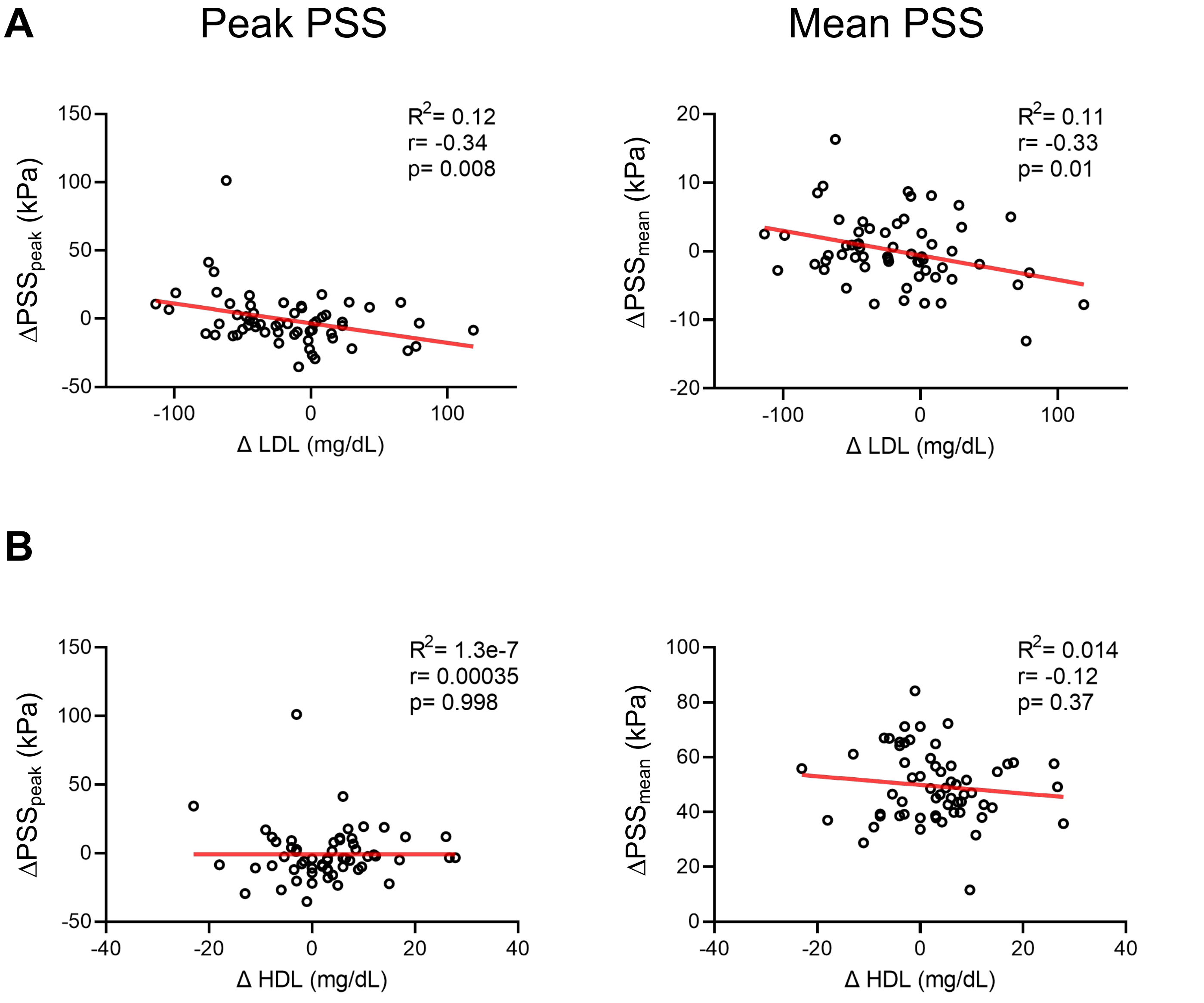


**Figure S2. Association between change in PSS and change in lipid levels.**
Linear correlation curves for change in peak (left) and mean PSS (right) with change in **(A)** LDL, **(B)** HDL. LDL or HDL changes are values for follow-up minus baseline, such that a higher negative value indicates a greater reduction from treatment. HDL= high-density lipoprotein; LDL= low-density lipoprotein; PSS = plaque structural stress.

# Figure S3

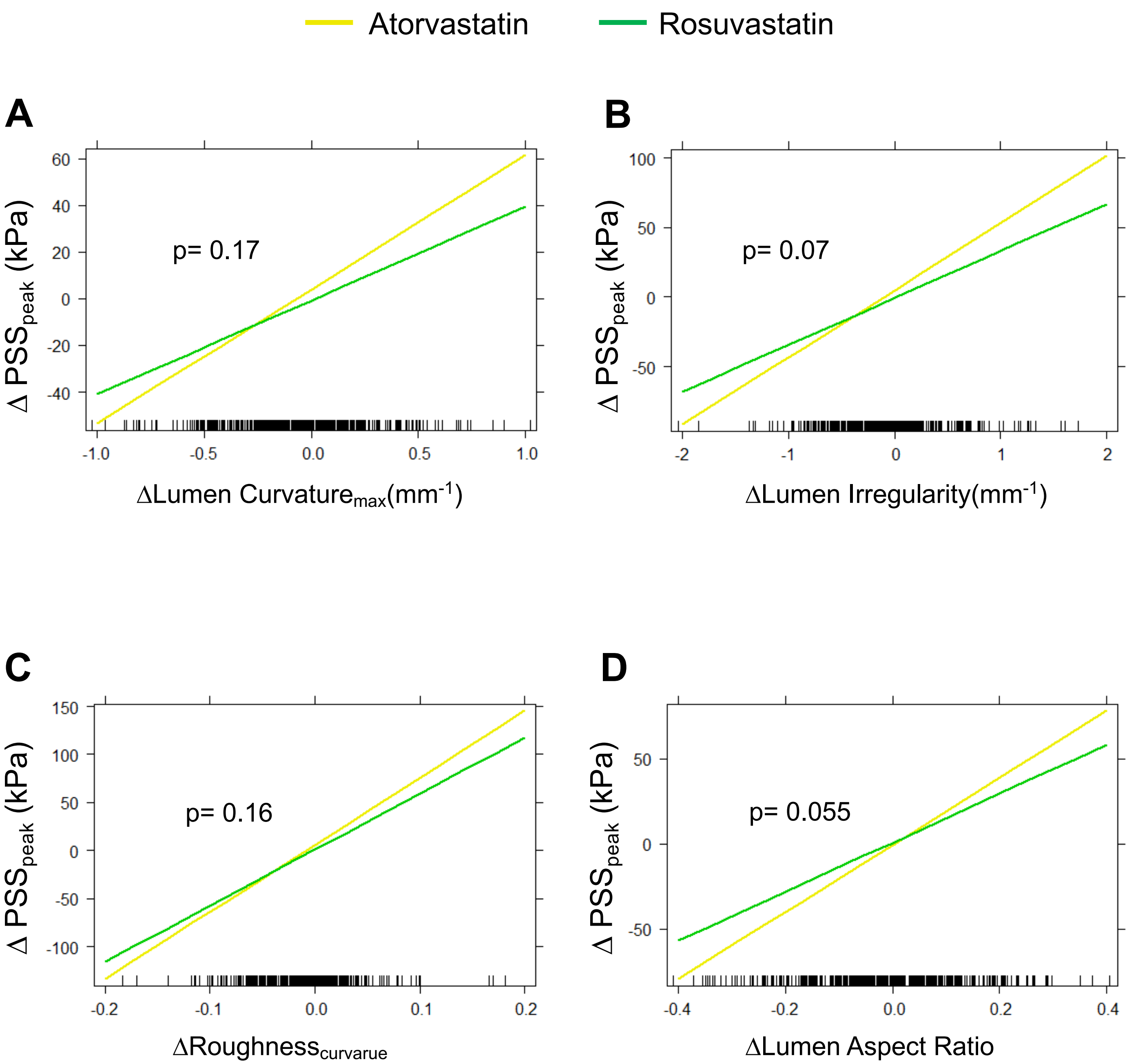


**Figure S3. Correlation between changes in peak PSS and lumen parameters in atorvastatin and rosuvastatin groups in plaques with baseline PB>60%.**
**(A)** maximum lumen curvature, **(B)** lumen irregularity, **(C)** lumen roughness **(D)** lumen aspect ratio. These regression slopes between the 2 high-intensity statin groups are similar ($p>0.05$).

**Supplemental References**


1. Ebenstein DM, Coughlin D, Chapman J, Li C, Pruitt LA. Nanomechanical properties of calcification, fibrous tissue, and hematoma from atherosclerotic plaques. *J Biomed Mater Res Part A* John Wiley & Sons, Ltd; 2009;**91A**:1028–1037.
2. Teng Z, Zhang Y, Huang Y, Feng J, Yuan J, Lu Q, Sutcliffe MPF, Brown AJ, Jing Z, Gillard JH. Material properties of components in human carotid atherosclerotic plaques: A uniaxial extension study. *Acta Biomater* Acta Materialia Inc.; 2014;**10**:5055–5063.
3. Teng Z, Sadat U, Li Z, Huang X, Zhu C, Young VE, Graves MJ, Gillard JH. Arterial Luminal Curvature and Fibrous-Cap Thickness Affect Critical Stress Conditions Within Atherosclerotic Plaque: An In Vivo MRI-Based 2D Finite-Element Study. *Ann Biomed Eng* 2010;**38**:3096–3101.
4. Akyildiz AC, Speelman L, Nieuwstadt HA, Brummelen H van, Virmani R, Lugt A van der, Steen AFW van der, Wentzel JJ, Gijsen FJH. The effects of plaque morphology and material properties on peak cap stress in human coronary arteries. *Comput Methods Biomech Biomed Engin* Taylor & Francis; 2016;**19**:771–779.
5. Teng Z, Sadat U, Ji G, Zhu C, Young VE, Graves MJ, Gillard JH. Lumen Irregularity Dominates the Relationship Between Mechanical Stress Condition, Fibrous-Cap Thickness, and Lumen Curvature in Carotid Atherosclerotic Plaque. *J Biomech Eng* 2011;**133**.
6. Teng Z, Degnan AJ, Sadat U, Wang F, Young VE, Graves MJ, Chen S, Gillard JH. Characterization of healing following atherosclerotic carotid plaque rupture in acutely symptomatic patients: an exploratory study using in vivo cardiovascular magnetic resonance. *J Cardiovasc Magn Reson* 2011;**13**:64.